New Thickness Control Process of Oxide Barrier for Nb-Based Tunnel Junctions

Ming-Jye Wang, Hong-Wen Cheng, Sing-Lin Wu, Pi-Kuang Chuan, and C. C. Chi

***Abstract*—The Nb-based superconductor-insulator-superconductor (*SIS*) tunnel junctions have been broadly used in many applications. The critical current density (J_C), one of the most important parameters of *SIS* tunnel junction, is usually controlled by the oxygen exposure (E_{O2}) of the Al oxidation process. R. E. Miller *et al.* demonstrated the relation between J_C and oxygen exposure using the SNEP process. However, the value of J_C still varies with Nb/AlO$_x$Al/Nb deposition system, even run-to-run process. A new AuAl$_2$/Al composite, instead of pure Al, has been used in the oxidation process. From the J_C-E_{O2} relation, we have demonstrated the oxidation rate of AuAl$_2$ is about 400 times lower than that of Al. Using AuAl$_2$ layer, two advantages are observed. 1) For low J_C tunnel junctions, the thickness of AlO$_X$, or J_C, can be controlled easily by inserting AuAl$_2$ layer as a blocking layer in oxidation process. 2) High quality factor tunnel junctions with $J_C > 100$ kA/cm^2 are achieved by oxidation of AuAl$_2$ layer directly.**

***Index Terms*—AuAl$_2$, critical current density, Josephson tunnel junction, oxygen exposure.**

I. Introduction

THE CRITICAL current density (J_C) of Nb-based *SIS* can vary several orders of magnitude without degrading junction's quality. There are still, however, two major problems in junction fabrication. The first one is the run-to-run variation of J_C in practical fabrication. The second one is the quality degradation of junction with ultrahigh J_C. Kleinsasser *et al.* [1] had compared the dependence of J_C on oxygen exposure (E_{O2}) in Nb/AlO$_x$/Nb tunnel junctions fabricated by many groups. Although there seems a universal dependence of J_C on E_{O2}, variation of J_C, fabricated by different groups, is observed. It indicates that the Al oxidation process is strongly dependent on the condition of fabrication system. Even for the same group, this variation still exists. For the ultrahigh J_C tunnel junction, Miller *et al.* [2], and Kleinsasser *et al.* [3] had reported Nb/AlO$_x$/Nb junctions with J_C higher than 10 kA/cm^2. However, their junctions have high sub-gap current. The junction degradation is attributed to naturally occurring defects in the barrier, like pin holes. To solve this problem, aluminum nitride has been tried as a tunnel barrier in the Nb-based junctions [3]. The quality factor of Nb/AlN/Nb junctions can be improved remarkably.

In this paper, we will demonstrate a new process by using Au–Al composite to solve both previous problems. We choose Au–Al composite because of two reasons. Firstly, Marinkovic *et al.* [4] reported that the interdiffusion between Au and Al proceeds even at room temperature in the thin film system. There is no need to do any further heat treatments during process. Thus it minimizes the modification of fabrication process. Secondly, Piao *et al.* [5] have reported that an AlO$_x$ layer can be formed on the surface of the AuAl$_2$ compound. Thus, this oxide layer can be used as a tunnel barrier. In addition, gold is inert to the oxygen. We believe that the oxidation rate of AuAl$_2$ should be much slower than that of pure Al. The oxygen exposure will be higher than that in the pure Al case for the same J_C. Therefore, the oxidation process can be easily controlled.

II. Experiments

A. Junction Fabrication

Nb-based junctions are fabricated by standard "self-alignment" method [6]. For conventional fabrication process, after 70 Å thick Al film is deposited, the surface is exposed to pure oxygen gas for oxide barrier growth. The oxide thickness can be controlled by oxygen pressure and exposure time. In our new process, an Al–Au–Al composite, instead of pure Al, of total 70 Å thickness is deposited consecutively. Before oxidation process, we wait 20 minutes for the inter-diffusion process between Au and Al. The position of the Au layer is varied to study its influence on oxidation process. The wafer is mounted on a pure copper plate is cooled by water-cooling system during whole process. The temperature is set at 15 °C for regular process and can be varied for studying the temperature effect on oxidation process.

B. Sample Analysis

The composition near the tunnel barrier is analyzed by electron microscope (AEM) and transmission electron microscope (TEM). The AEM and TEM sample have similar structure to the real junction except for 70 Å of Nb, instead of 1000 Å Nb. The I–V characteristics of tunneling junctions are measured by the standard four-probe method. The critical current density of sample is obtained by using the theoretical formula,

$$I_C = \left(\frac{\pi\Delta(T)}{2eR_n}\right)\tanh\left(\frac{\Delta(T)}{2k_BT}\right), \qquad (1)$$

where $\Delta(T)$ is the measured superconducting energy gap at temperature T and R_n is the normal state resistance of the junc-

Manuscript received August 6, 2002. This work was supported in part by the National Science Console, Taiwan under Grant NSC89-2212-M-007-098.

M.-J. Wang and H.-W. Cheng are with the Institute of Astronomy and Astrophysics, Academia Sinica, Taipei, 104, Taiwan, R.O.C. (e-mail: mingjye@asiaa.sinica.edu.tw; hwcheng@asiaa.sinica.edu.tw).

S.-L. Wu and C. C. Chi are with the Physics Department of National Tsing-Hua University, Shin-Chu, 300, Taiwan, R.O.C. (e-mail: cchi@phys.nthu.edu.tw).

P.-K. Chuan is with the Physics Department of National Tsing-Hua University, Shin-Chu, 30043, Taiwan, R.O.C.

Digital Object Identifier 10.1109/TASC.2003.814165

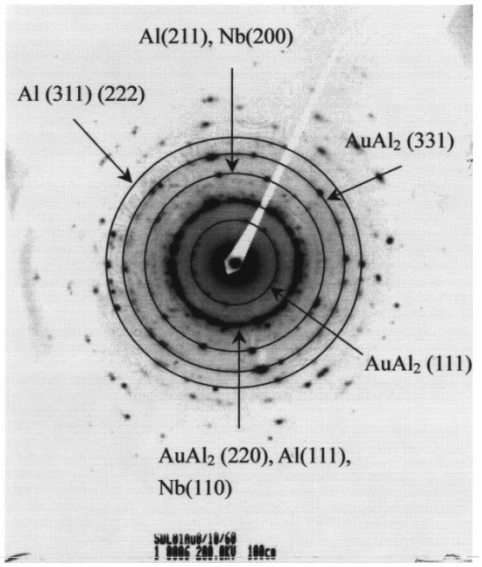

Fig. 1. TEM diffraction pattern of sample with Au/Al of 10 Å/60 Å. The electron energy is 200 keV and sample-detector distance is 10 cm. We can identify the diffraction plane from the relation $r = \lambda L/d$, where r is the radius of diffraction pattern, L is the sample-detector distance, λ is the electron wavelength, and d is the plane distance.

tion. However, for ultra-high J_C sample, its sub-gap leakage current becomes larger and this formula cannot be used in this case. We estimate their J_C from the I–V curve directly.

III. Results and Discussions

In our samples, we keep the Au/Al ratio in Au–Al composite at 1 : 6, which is in Al rich region. According to the G. Majni's result [7], most of Au atoms react with adjacent Al atoms and form $AuAl_2$ compound. Fig. 1 is the plane view of TEM pattern near the tunnel barrier with Au/Al = 10 Å/60 Å structure. The electron energy is 200 keV, corresponding to electron wavelength, λ, of 0.0251 Å. Sample-detector distance is 10 cm. We can identify the diffraction plane from the relation $r = \lambda L/d$, where r is the radius of diffraction pattern, L is the sample-detector distance, λ is the electron wavelength, and d is plane distance. The structure of Nb is bcc with lattice constant of 3.31 Å. And the structure of Al and $AuAl_2$ is fcc and diamond with lattice constant of 4.05 Å and 6 Å, respectively. In Fig. 1, the first ring is the diffraction pattern of $AuAl_2$ (111) plane. The second ring consists of $AuAl_2$ (220), Nb (100) and Al (100). The fifth ring is from $AuAl_2$ (311) and $AuAl_2$ (222). This result indicates that $AuAl_2$ is the major phase of Au–Al compound in our sample.

To study the oxidation of $AuAl_2$, instead of depositing pure $AuAl_2$, we use an Au/Al composite with thickness of 10 Å/60 Å in our junction fabrication process. The purpose of this structure is to keep the good wetting property between Nb and Al interface. The Au and Al forms $AuAl_2$ on the surface of the composite. Similar to the pure Al process, the $AuAl_2$ surface is exposed to pure oxygen to grow the barrier oxide layer. Fig. 2 shows the oxygen exposure dependence of J_C. The squares are the data from the new $AuAl_2$–Al process. For comparison, we also plot the data from the conventional pure

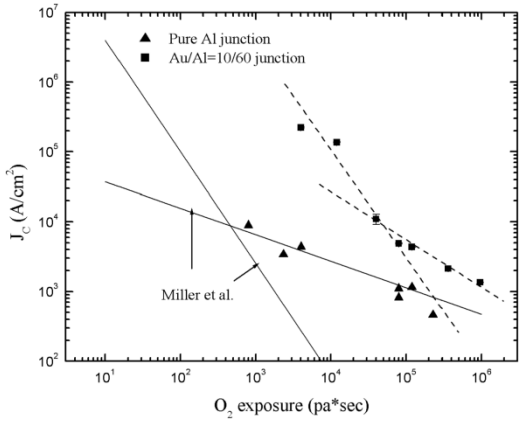

Fig. 2. The oxygen exposure dependence of J_C. The squares are the data from the new barrier materials and the triangles are the data from conventional pure Al process. The solid line is extracted from Miller's result [2] and the dash line is an approximate plot guided by eyes.

Al process including our result (triangles), and an empirical fitting of $J_C(E_{O2})$ given by Miller *et al.* [2] (solid lines). The J_C of these two systems, clearly, have similar oxygen exposure dependence, except for shifting to higher exposure region in $AuAl_2$–Al samples. For the same J_C value, the oxygen exposure of $AuAl_2$ is about one (low J_C region) to two (high J_C region) orders of magnitude higher than that in pure Al case. It implies that the oxidation rate of $AuAl_2$ is about 10 to 100 times slower than that of pure Al.

It is generally believed that the initial oxidation growth on Al is controlled by the collision rate of oxygen molecules and the surface reaction process. This accounts for the solid line representing higher J_C in Fig. 2. After a thin layer of Al_2O_3 has grown, the oxide growth rate becomes much slower due to the thermal activated oxygen or aluminum diffusion through the Al_2O_3 layer. It explains the much slower dependence of J_C on oxygen exposure in higher exposure region. However, in $AuAl_2$ system, we believe that Al atoms must diffuse to the surface before the regular oxidation procedure. Usually, this kind of diffusion rate is much lower than the initial oxidation rate and comparable to the oxygen or aluminum diffusion rate through the thin Al_2O_3 layer. From Fig. 2, we can roughly estimate that the Al diffusion rate in $AuAl_2$ is about 100 times lower than the initial oxidation rate of Al and about 10 times lower than the oxygen or aluminum diffusion rate through the thin Al_2O_3 layer.

Because of the low oxidation rate, a thin $AuAl_2$ layer can be used for the oxide growth control in junction fabrication. We have demonstrated ultrahigh J_C, >100 kA/cm^2, tunnel junctions [8]. Typical I–V characteristic is shown in Fig. 3. The quality factor, defined by the ratio of sub-gap resistance and normal state resistance, is about 2.78, which is higher than that of junctions with J_C at 25 kA/cm^2 reported in [2] and 18.4 kA/cm^2 reported in [3] for AlO_x barrier junctions. The quality degradation of SIS junctions with ultrahigh J_C is usually attributed to pin holes in thin oxide barrier. The formation of pin hole is related to the coverage of oxide on the Al surface. Usually, higher oxygen exposure, i.e., higher total oxygen molecule collision events, will reduce the formation of pin holes. For the $AuAl_2$ oxidation process, the oxidation possibility of Al atoms, which diffuse from interior of $AuAl_2$ to the surface, are about

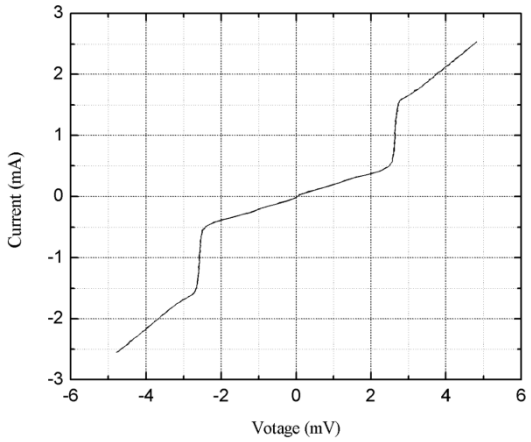

Fig. 3. I–V curve of ultrahigh J_C junction. The junction area is about 1 μm^2 and the barrier is formed by oxidation of $AuAl_2$ directly. The supercurrent is suppressed by applying an appropriate amount of magnetic fields. The quality factor, R_g/R_n is 2.78, where R_g is the sub-gap resistance at 2 mV and R_n is the normal state resistance of junction.

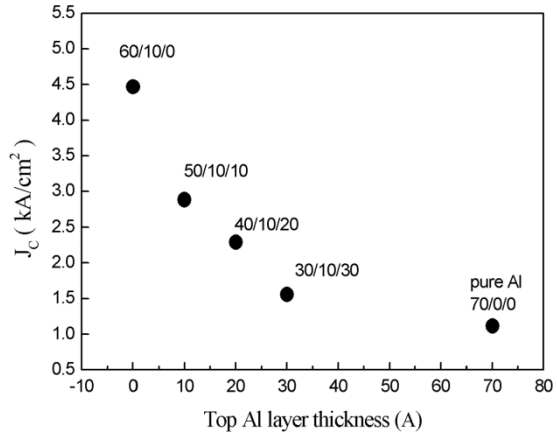

Fig. 4. The dependence of J_C on the top Al layer thickness. All junctions have same oxygen exposure, 1000 mtorr × 15 minutes. The junction with pure Al layer is marked at position of 70 Å. The value of J_C increases remarkably as the top Al thickness decreases.

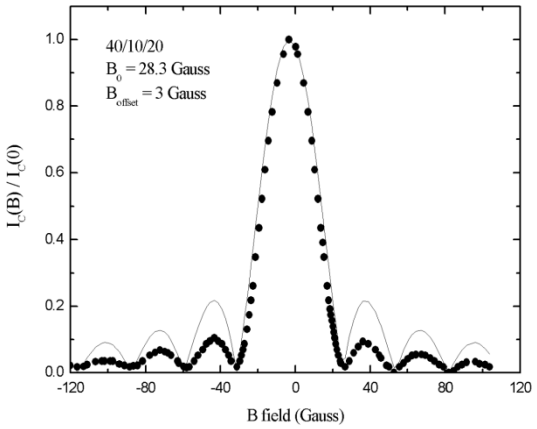

Fig. 5. Normalized I_C-B curve. The solid dots are the experimental data and solid line is the best fit using the standard magnetic modulation formula. The good fit of I_C-B curve shows good uniformity of oxide barrier in our new process.

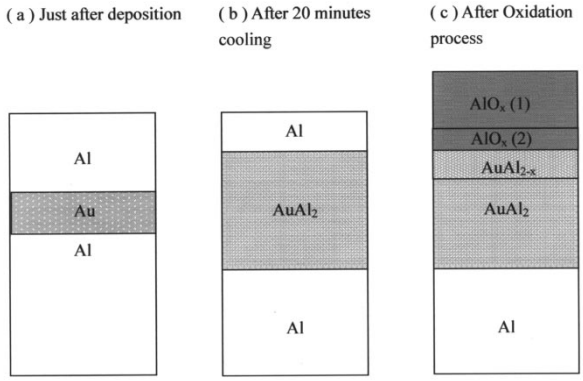

Fig. 6. A schematic model of oxidation process under high oxygen exposure. The process can be described as (a) Al/Au/Al multilayer deposition, (b) diffusion between Au and adjacent Al, (c) oxidation of top Al and $AuAl_2$. The oxygen exposure is assumed long enough to oxidize the Al above $AuAl_2$ layer completely.

100 times lower than that of pure Al case. Thus, the number of pin hole can be reduced significantly.

Another possible application of low oxidation rate of $AuAl_2$ is on total thickness control of oxide barrier. By inserting a thin $AuAl_2$ layer in Al, i.e., Al–$AuAl_2$–Al multilayer, for *SIS* junction fabrication, this $AuAl_2$ layer could be a blocking layer during the oxidation process and limit further oxidation. Fig. 4 shows the dependence of J_C on the top Al thickness, i.e., the position of $AuAl_2$ layer, in the Al–$AuAl_2$–Al composite. We keep the total thickness of composite same as the pure Al case, 70 Å, which is marked at 70 Å in the plot for comparison. All samples have same oxygen exposure, 15 000 mtorr-min. The J_C increases markedly as the $AuAl_2$ layer is moved closed to the surface. It indicates that the oxidation process is strongly limited by $AuAl_2$ layer after the top Al layer is fully oxidized for this particular structure and oxygen exposure. The AlO_x thickness is controlled by the position of $AuAl_2$ blocking layer.

Fig. 5 shows the normalized I_C versus magnetic field. The solid dots are the experimental results and the solid line is the best fit using standard magnetic field modulation formula, $|\mathrm{Sin}(B-B_{offset})/B_o|$. The $I_C(B)$ is normalized to the maximum observed I_C, which is at a magnetic field of 3 Gauss. This offset magnetic field is due to the flux trapping near the junction. The experimental results can be fitted well with a magnetic field period of 28.3 Gauss. Compared to the theoretical value, the reduction of measured I_C is attributed to the noise of the measuring system. It is well known that the fitting of I_C-B curve is a measure of the uniformity of tunneling barrier. The good fit of $I_C(B)$ curve demonstrates the good uniformity of the oxide barrier in our process.

Fig. 6 shows the oxidation process model for our new process. The Al/Au/Al structure is deposited initially, Fig. 6(a). After cooling for 20 minutes, the Au atoms react with adjacent Al and form $AuAl_2$ layer, Fig. 6(b). In the case of light oxygen exposure or thick top Al layer, the Al layer above the $AuAl_2$ layer is not completely oxidized. Thus, the AlO_x growth rate is similar to a pure Al oxidation process. On the other hand, the oxidation process should include the oxidation mechanisms of $AuAl_2$ for sufficient long oxygen exposure or very thin top Al layer. In this case, all the Al on the top of $AuAl_2$ layer will be

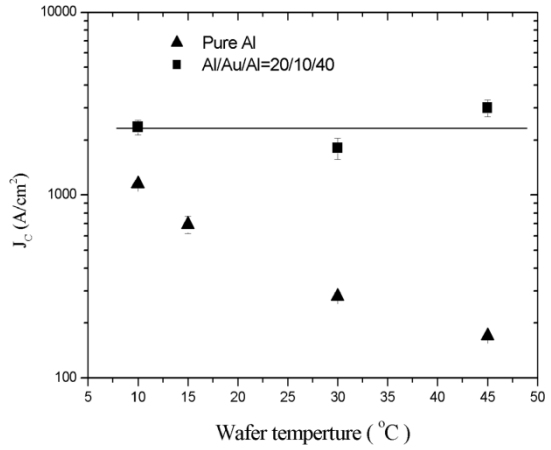

Fig. 7. The dependence of J_C on wafer temperature. All samples have same oxygen exposure, 1000 mtorr × 15 minute. The value of J_C decreases in pure Al process (squares) as wafer temperature increases. However, the value of J_C is almost independent of the wafer temperature, for the Al/Au/Al samples.

oxidized and form AlO_x(1) layer. In addition, a thin Al layer, diffusing from $AuAl_2$, also be oxidized and form an AlO_x(2) layer. The final structure is shown in Fig. 6(c). Because of the low oxidation rate of $AuAl_2$, the thickness of AlO_x(2) is only a minor contribution to total oxide thickness. Thus, the AlO_x thickness will most likely be dominated by the thickness of the Al layer. When the top Al layer thickness is decreased, the AlO_x thickness will be decreased for same oxygen exposure condition and, thus, J_C will be increased, as shown in Fig. 4.

As mentioned above, the oxidation process is dominated by oxygen or aluminum thermally activated diffusion through the AlO_x layer. In practical fabrication, the temperature of wafer could be increased by plasma heating during deposition. It sometimes causes a problem for the reproducibility of J_C if the thermal anchoring is not sufficient. This problem could be solved by our new fabrication technique. Fig. 7 shows the dependence of J_C on wafer temperature during the oxidation process. The Al/Au/Al composite thickness is 20 Å/10 Å/40 Å and the oxygen exposure is 15 000 mtorr-min, and the temperature range is 10 °C to 45 °C. For the pure Al process, the value of J_C decreases quickly as wafer temperature increases. J_C varies by about a factor of ten for wafer temperatures between 10 °C and 45 °C. This is consistent with a thermal activation process. For this new process, J_C is almost independent on the wafer temperature, within 20% variation. This result clearly reveals the benefit of our new process. The thickness of AlO_x can be controlled more easily in practical fabrication.

IV. Conclusion

In summary, we have demonstrated a new process to control the oxide barrier thickness for Nb-based tunnel junction by adding a thin Au layer. From the modulation of I_C by magnetic field, our junctions have good uniformity of oxide barrier. High quality junctions with ultrahigh current density, formed by oxidizing $AuAl_2$ as the tunnel barrier, were achieved. We have also demonstrated the capability of oxide thickness control by using the new structure of Al/$AuAl_2$/Al. In addition, the value of J_C is almost independent of the wafer temperature during oxidation process. These benefits could improve the J_C control in practical junction fabrication. However, we should point out that sub-gap structure of I–V curve is observed in these samples. Further experiments are necessary to understand whether this sub-gap structure is an intrinsic property of this kind of junction, or it can be improved by modifying the fabrication process.

Acknowledgment

The authors would like to thank A. Kleinsasser for his helpful discussion.

References

[1] A. W. Kleinsasser, R. E. Miller, and W. H. Mallison, "Dependence of critical current density on oxygen exposure in Nb–AlOx–Nb tunnel junctions," *IEEE Trans. Appl. Supercond.*, vol. 5, no. 1, pp. 26–30, March 1995.

[2] R. E. Miller, W. H. Mallison, A. W. Kleinsasser, K. D. Delin, and E. M. Macedo, "Niobium trilayer Josephson tunnel junctions with ultrahigh current densities," *Appl. Phys. Lett.*, vol. 63, pp. 1423–1425, Sept. 1993.

[3] A. W. Kleinsasser, W. H. Mallison, and R. E. Miller, "Nb/AlN/Nb Josephson junctions with high critical current density," *IEEE Trans. Appl. Supercond.*, vol. 5, no. 2, pp. 2318–2321, June 1995.

[4] Z. Marinkovic and V. Simic, "Room temperature interactions in Au/Metal and Al/Metal thin film couples," *Thin Solid Films*, vol. 75, pp. 229–235, 1981.

[5] H. Piao and N. S. McIntyre, "High resolution XPS studies of thin film gold-aluminum alloy structures," *Surface Science*, vol. 421, pp. L171–L176, 1999.

[6] M. J. Wang, H. W. Cheng, Y. H. Ho, and C. C. Chi, "Low noise Nb-based SIS mixer for sub-millimeter wave detection," *J. Phys. Chem. Solids*, vol. 62, p. 1731, 2001.

[7] G. Majni, G. Ottaviani, and E. Galli, "AuAl compound formation by thin film interactions," *J. Crystal Growth*, vol. 47, p. 583, 1979.

[8] M. J. Wang, P. K. Chuang, S. L. Wu, H. W. Cheng, and C. C. Chi, "A new barrier material for ultrahigh current density Josephson tunnel junctions," *Sing. J. Phys.*, vol. 18, no. 1, pp. 221–226, 2002.